The Performance of an Aerodynamic Efficiency of Bullet-Nose Vs Chisel-Nose Design Parameters in F1 in Schools Racing Competitions

Masjuri Musa @ Othman[1], Soh Tien Een[2]

Fakulti Teknologi dan Kejuruteraan Mekanikal, Universiti Teknikal Malaysia Melaka, 75450 Ayer Keroh, Melaka, Malaysia

DOI: https://doi.org/10.47772/IJRISS.2026.100800474

Received: 23 August 2026; Accepted: 28 August 2026; Published: 08 September 2026

ABSTRACT

This study investigates the aerodynamic performance of bullet and chisel nosecone design for F1 in Schools racing cars with different parameters. This work applies to a systematic concept generation process using a morphological chart method to define and cross-combine nosecone parameters variations within the allowable limits by following the official 2025 F1 in Schools Technical Regulations. All nosecone models were developed by using SolidWorks software and comprehensive airflow simulations via ANSYS Workbench software fluent analysis system, utilizing the steady state turbulence model at a 22m/s velocity. A total of 325 design (25 model for bullet and 300 model for chisel nosecone) were evaluated. The results indicate that the bullet nosecone profile exhibits a highly linear drag trend, chisel nosecone profile exhibits a highly non-linear with parametric coupling effect. Ultimately, bullet nosecone is determined to be the optimal structure for maximizing the aerodynamic performance based on the bullet nosecone drag force and drag coefficient results better than chisel nosecone 10% plus.

Keywords: F1 in Schools; bullet and chisel nosecone; aerodynamic performance; linear and non-linear drag trend; parametric coupling effect.

INTRODUCTION

The F1 in Schools racing competition is a program that is based on engineering technology. The F1 in Schools racing car size is 1:24 to the real F1 car [1]. The speed test track for F1 in Schools races is 20 meters long. The car is powered by compressed carbon dioxide cylinder mounted at the rear of the car. Racing results are often decided by a fraction of a second.

The front nosecone as the primary leading-edge structure in contact with the airflow, plays an important role in the initial flow separation and stagnation pressure. Aerodynamic efficiency in F1 in schools racing cars is characterized by the minimization of the drag force, which acts opposed to the car motion. Therefore, an efficient nosecone geometry can reduce drag force by increasing smoother airflow opposed to the car [2].

Previous research more focused on the full-scale F1 in schools car aerodynamic optimization, especially optimization on components such as front wing, sidepods and diffusers. The research specifically investigating the impact of nosecone geometry is limited. Furthermore, comparative studies of bullet nosecone and chisel nosecone are also scarce.

Therefore, this research utilized computational fluid dynamics (CFD) simulations in ANSYS Workbench software fluent analysis system to investigate the aerodynamic performance of bullet nosecone and chisel nosecone designs. A total of 325 nosecone models were developed and evaluated, to evaluate drag force and drag coefficient. The goal was to determine the nosecone parameters with the highest aerodynamic efficiency in F1 in Schools applications.

INTERNATIONAL JOURNAL OF RESEARCH AND INNOVATION IN SOCIAL SCIENCE (IJRISS)
ISSN No. 2454-6186 | DOI: 10.47772/IJRISS | Volume X Issue VIII August 2026

METHODOLOGY

Method that is used as a guide for this study is shown in the flowchart in Figure 2.1.

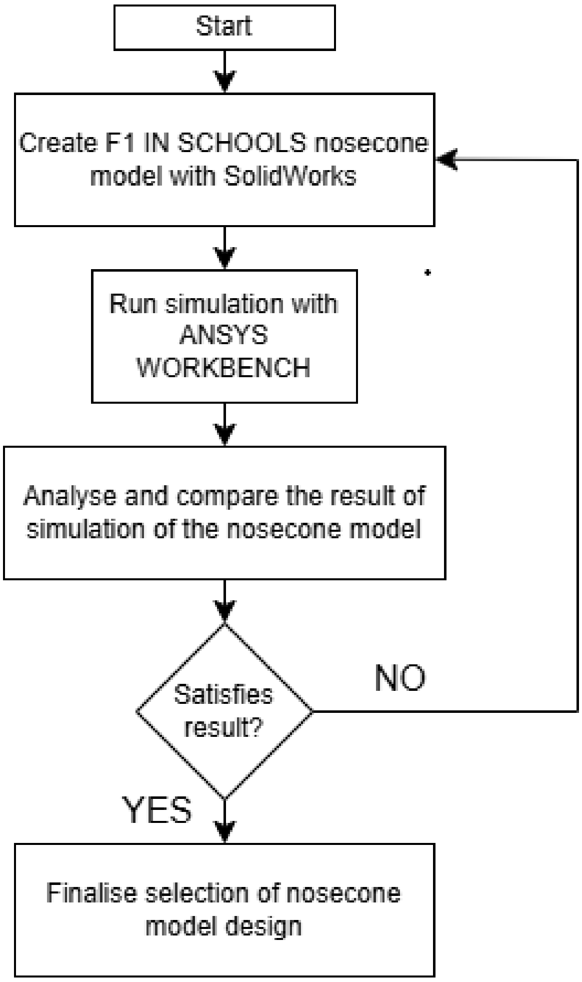

Figure 2.1: Methodology flowchart

Parameters of nosecone design

Table 2.1 shows the parameters of chisel nosecone design and Table 2.2 shows the parameters of bullet nosecone design. Based on using morphological chart method, a total of 300 models of chisel nosecone will be created and 25 models of bullet nose cone.

Table 2.1: Parameters of chisel nosecone design

Nosecone model Isometric view	Edge Treatment Side-light bottom view	Nose tip length Isometric view	Angle Side view
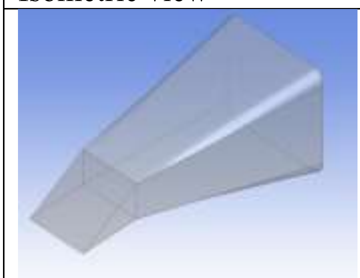 Model A	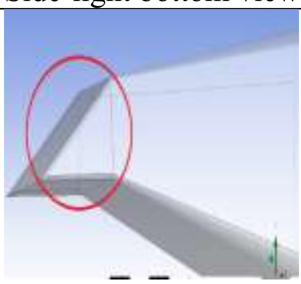 2A: Filleted Edge	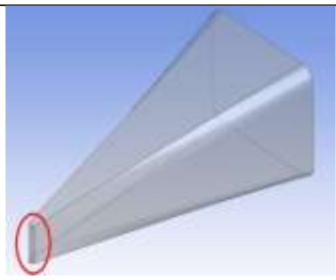 3A: 1mm	 4A: +9 degree

INTERNATIONAL JOURNAL OF RESEARCH AND INNOVATION IN SOCIAL SCIENCE (IJRISS)
ISSN No. 2454-6186 | DOI: 10.47772/IJRISS | Volume X Issue VIII August 2026

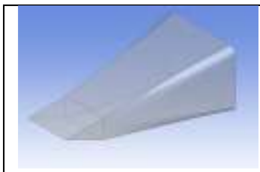 Model B	 2B: Sharp Edge	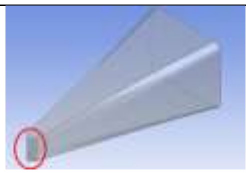 3B: 2.5mm	 4B: +4.5 degree
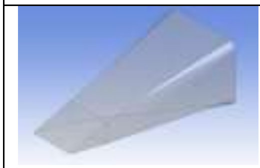 Model C	 2C: Chamfer Edge	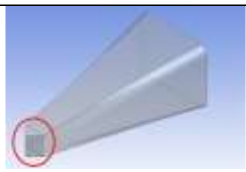 3C: 5mm	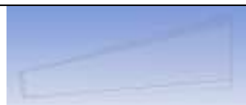 4C: -9 degree
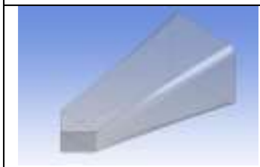 Model D		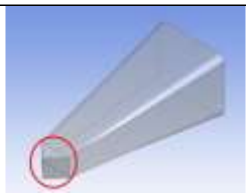 3D: 7.5mm	 4D: -4.5 degree
		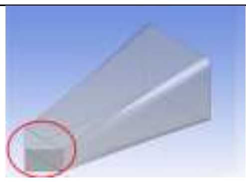 3E: 10mm	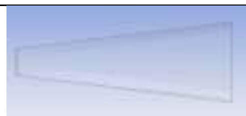 4E: 0 degree

Table 2.2: Parameters of bullet nosecone design

Nose tip radius Side view	Angle Side view
 Model A: 2mm	 2A: +9 degree
 Model B: 4mm	 2B: +4.5 degree
 Model C: 6mm	 2C: -9 degree
 Model D: 8mm	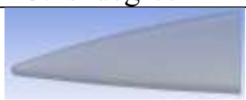 2D: -4.5 degree
 Model E: 10mm	 2E: 0 degree

ISSN No. 2454-6186 | DOI: 10.47772/IJRISS | Volume X Issue VIII August 2026

ANSYS Workbench software simulation setup

Figure 2.2 shows that the process flowchart for obtaining the end results.

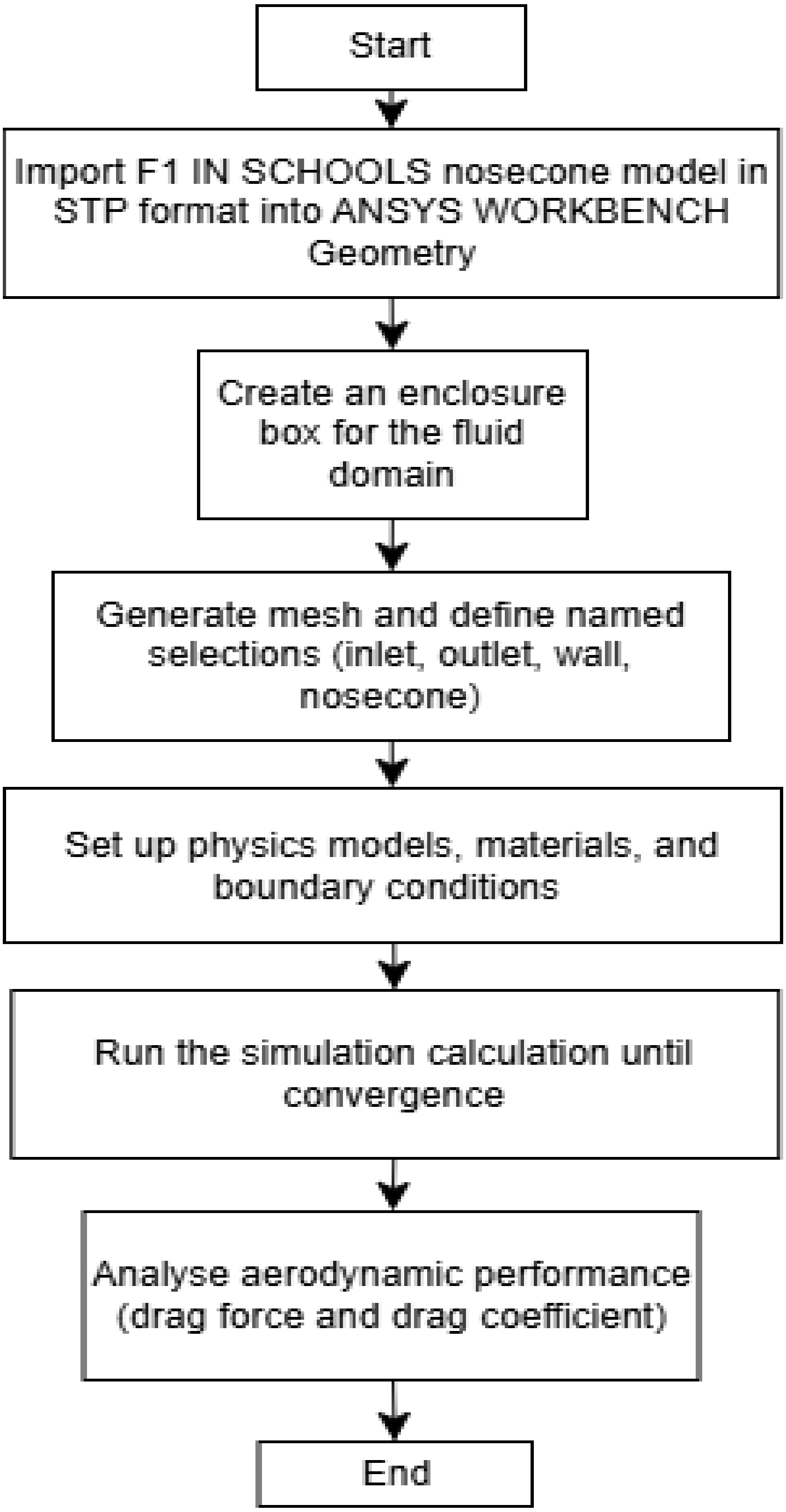

Figure 2.2: Flowchart of the ANSYS Workbench simulation software

To ensure the aerodynamic simulations have the same accuracy for all nosecone models, a consistent computational domain and boundary condition configuration is applied to all nosecone models in the simulation setup.

The enclosure which is virtual wind tunnel was generated in ANSYS WORKBENCH geometry Design Modeler software. The flow domain boundaries were defined using a non-uniform cushion dimensions tailored to the F1 IN SCHOOLS regulation. With the principal flow development aligned along the Z-axis as shown in Figure 2.3.

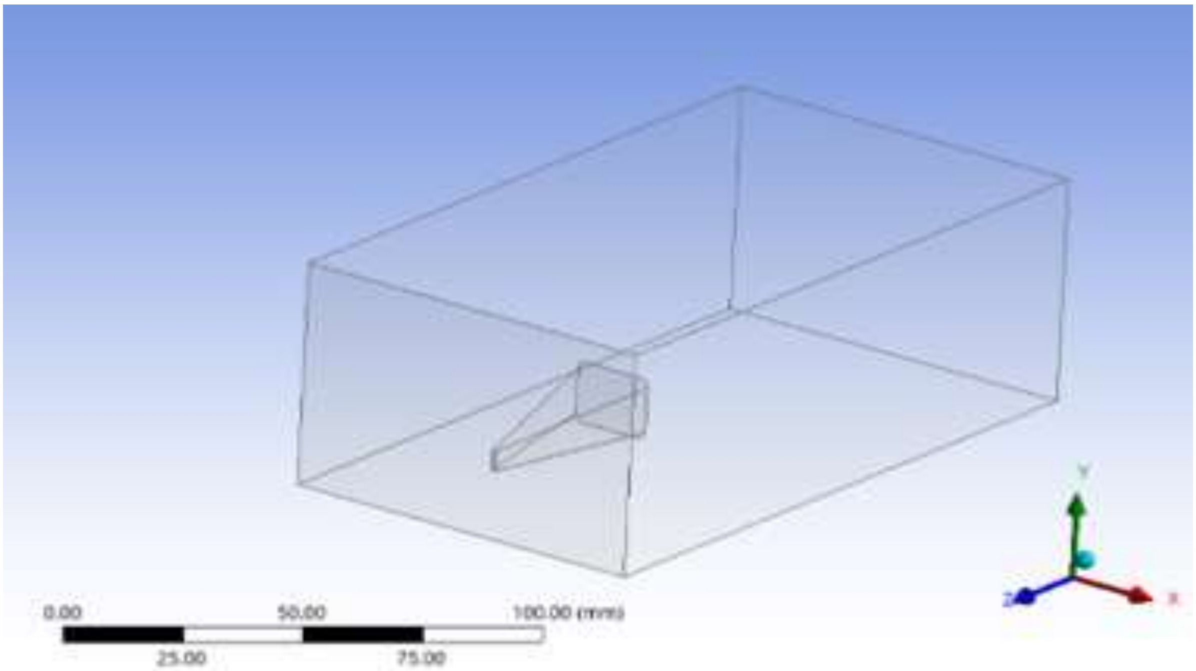

Figure 2.3: Isometric view - detail direction aligned of the nosecone

- Lateral Clearance (X-axis): ±33.5mm from the model symmetry plane.
- Vertical Clearance (Y-axis): +30mm above and -10mm below the model base.
- Streamwise Clearance (Z-axis): +10mm upstream (inlet distance) and -100mm downstream (outlet wake expansion region).

Meshing module with a physics preference set to CFD and solver preference to Fluent. The precise meshing parameters applied to balance computational economy and spatial resolution are outlined in Table 2.3 below.

Table 2.3: Mesh properties

Important parameters of the mesh	**Description**
Element Size	Set to 5mm to adequately capture the global flow characteristics.
Sizing	Enabled adaptive sizing with fine span angle centre to ensure high smoothing to transition elements smoothly near high-curvature geometric transitions of the nosecone.
Inflation	Use automatic inflation with program controlled to resolve the high-velocity gradients within the aerodynamic boundary layer on the nosecone surface.

The physical boundary types and properties specified for the simulation runtime domain are summarized in Table 2.4 below.

Table 2.4: Simulation properties

Category	**Parameters**	**Configured Specification/ Value**	**Description**
Physics and Turbulence	Solver Type	Pressure-Based	Suitable for low-speed incompressible external aerodynamics in nosecone.
	Time Formulation	Steady	
	Turbulence	$K-\omega$ turbulence	Increases the performance of boundary layer that

ISSN No. 2454-6186 | DOI: 10.47772/IJRISS | Volume X Issue VIII August 2026

	Model		is affected by adverse pressure gradient. Suitable to use for all boundary layer included at boundary that is dominated by viscosity [3].
	Near-Wall Treatment	Enhanced Wall Treatment	Combines a blended law of the wall formulation to highly resolve near wall viscous sublayers [4].
	Fluid Material	Air	Standard fluid working medium with constant 1.225kg/m³.
Boundary Conditions	Domain Inlet	Velocity-Inlet	
	Velocity Magnitude	22m/s	
	Flow Direction Vector	Global Coordinate: (X=0, Y=0, Z=-1)	Forces the uniform freestream air to flow directly parallel to the negative Z-axis.
	Domain Outlet	Pressure-Outlet (0 Pa Gauge Pressure)	Simulates the ambient atmospheric pressure exit condition to prevent backflow errors.
	Nosecone Surface	Stationary Wall (No-Slip condition)	Enforces a zero-velocity boundary condition at the nosecone skin to capture friction drag.
	Enclosure Outer Walls	Stationary Wall (Symmetry condition)	Eliminates artificial wall friction on the wind tunnel boundary to mimic open-air testing.
Solver Controls	Max Allowed Iterations	100	Limits the solver computational runtime per design case.

To evaluate aerodynamic performance of the proposed nosecone designs, the aerodynamic drag force and drag coefficient are calculated based on simulated fluid-structure interactions. The mathematical relationship governing the aerodynamic drag is expressed as follows:

$$F_D = \frac{1}{2}\,\rho\, C_D A V^2$$

- F_D *is the drag froce*
- C_D *is the drag coefficient*
- A is the reference area
- ρ is the density of the medium (Air)
- V is the flow velocity relative to the object

RESULTS AND DISCUSSION

Based on the simulation results, Figure 3.1 and Figure 3.3 known that modelA_2E achieved the best aerodynamic performance among all bullet nosecone models, with a drag force 0.037223394N and a drag coefficient 0.49793977. The smooth and streamlined shape of the bullet nosecone helped the airflow move more smoothly around the model skin, reducing airflow separation and aerodynamic drag. Based on the results extracted from Figure 3.2 and Figure 3.4, ModelD_2A3C4E achieved the best aerodynamic performance with the drag force 0.041642349N and drag coefficient 0.5202595. This model was the best design for chisel nosecone model. The related model produced the lowest drag coefficient among all tested designs, mean that provided better aerodynamic efficiency and smoother airflow behavior.

ISSN No. 2454-6186 | DOI: 10.47772/IJRISS | Volume X Issue VIII August 2026

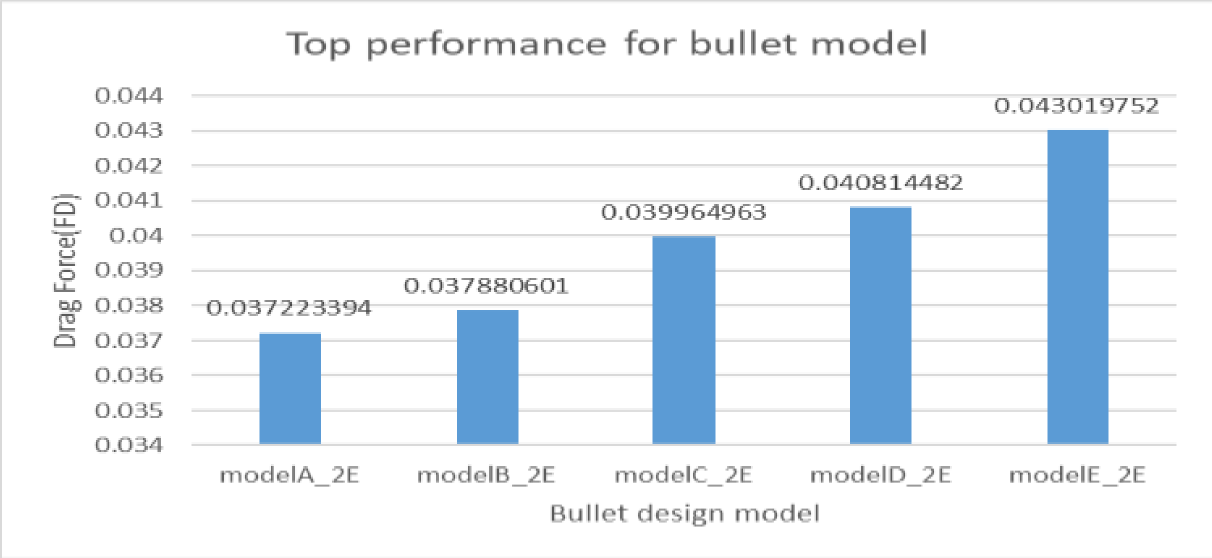

Figure 3.1: Top performance drag force for bullet models.

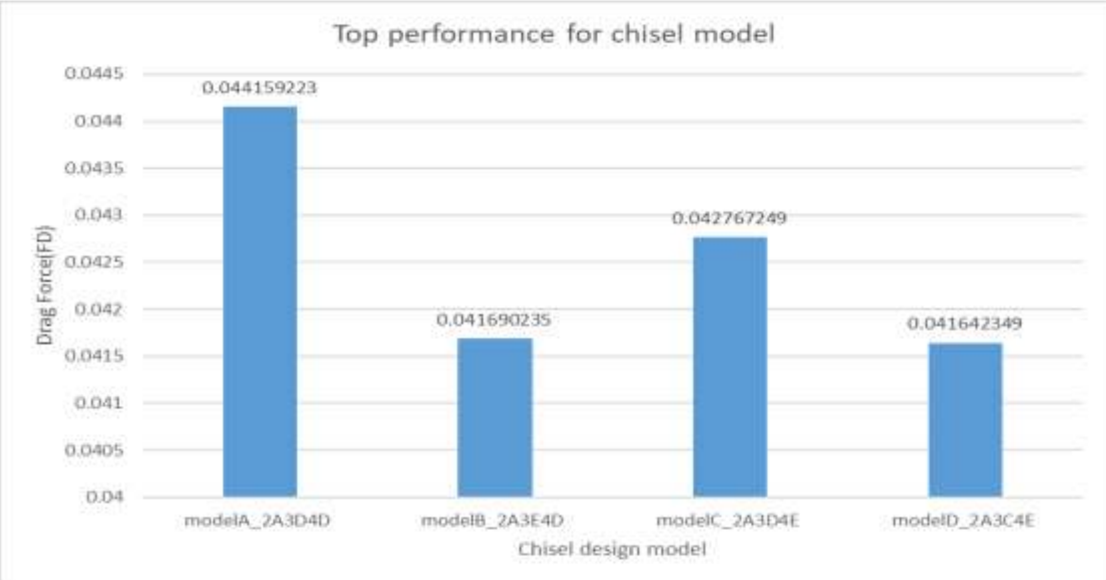

Figure 3.2: Top performance drag force for chisel models.

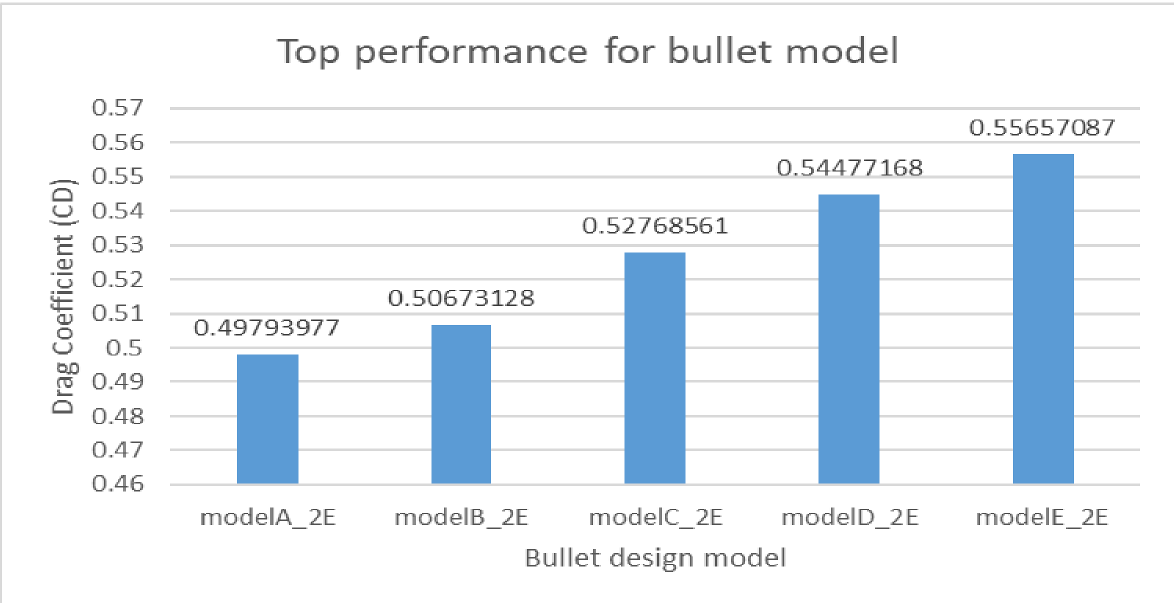

ISSN No. 2454-6186 | DOI: 10.47772/IJRISS | Volume X Issue VIII August 2026

Figure 3.3: Top performance drag coefficient for bullet models.

Figure 3.4: Top performance drag coefficient for chisel models.

For the bullet nosecone model, Table 3.1 and Table 3.2 show that the results of the bullet nosecone were selected to explain the quantification because of a consistent trend in aerodynamic performance was observed regarding the parameter modifications. The parameter 2A and 2C repeatedly yield the highest drag force on every model. However, parameter 2E consistently achieves the lowest level on every model. This behavior proves that the aerodynamic drag force is highly sensitive to the nosecone argle, indicating that an optimized angle can substantially reduce the drag force acting on the object surface.

Table 3.2 clearly shows both drag force and drag coefficient increase as the tip radius increases. This clearly demonstrates increased tip radius leads to a larger stagnation region and more intense airflow acceleration. The apex in front of the nose tip is called stagnation point, where the airflow pressure is greatest. A larger radius means a more rounded nosecone tip, which results in a larger high-pressure stagnation point region directly facing the airflow. Simultaneously, the airflow is forced to accelerate sharply as it bypasses this large arc, causing boundary layer instability as it bypasses this large arc, thus causing drag force and drag coefficient to gradually increase when tip radius increases.

Table 3.1 and Table 3.2 demonstrate that the nose tip angle represented a dominant role in governing the global flow structure around the nosecone. Variations in the angle directly alter the local pressure distribution and flow trajectories. A change of the angle can shift the positions of flow separation and reattachment, thereby explaining why different angles do not exhibit a simple linear relationship in drag force and drag coefficients, as each angle parameter essentially creates a distinct aerodynamic regime.

Table 3.1: Bullet nosecone results with constant tip radius and varies of angles.

NO	MODEL	FRONTAL AREA	DRAG FORCE	DRAG COEFFICIENT
1	modelA_2A	0.000272521	0.044960371	0.55651669
2	modelA_2B	0.000252167	0.043172877	0.5775264
3	modelA_2C	0.000273229	0.046208417	0.57048312
4	modelA_2D	0.000252167	0.043550053	0.5825719
5	modelA_2E	0.000252167	0.037223394	0.49793977

ISSN No. 2454-6186 | DOI: 10.47772/IJRISS | Volume X Issue VIII August 2026

Table 3.2: Bullet nosecone results with constant angle and varies of tip radius.

NO	MODEL	FRONTAL AREA	DRAG FORCE	DRAG COEFFICIENT
1	modelA_2E	0.000252167	0.037223394	0.49793977
2	modelB_2E	0.000252167	0.037880601	0.50673128
3	modelC_2E	0.000255478	0.039964963	0.52768561
4	modelD_2E	0.000252725	0.040814482	0.54477168
5	modelE_2E	0.000260733	0.043019752	0.55657087

Table 3.3 to Table 3.6 demonstrates upon evaluation of the comprehensive datasets across all 300 chisel nosecone parameters, the resulting drag force and drag coefficient do not exhibit a simple monotonic or linear trend. Result outputs exhibit a highly dispersed and fluctuating trend under different parameter combinations. From an aerodynamic perspective, this lack of a single linear model indicates a severe parametric coupling effect among the four geometric variables. When these parameters are used in combination, the flow field around chisel nosecone behaves as a highly nonlinear system and its aerodynamic efficiency depends on the synergistic effect of all parameters, rather than any single isolated parameter.

Table 3.3: Chisel nosecone results with varies of models

NO	MODEL	FRONTAL AREA	DRAG FORCE	DRAG COEFFICIENT
1	modelA_2A3C4E	0.000269286	0.045798685	0.57370451
2	modelB_2A3C4E	0.000269286	0.047017632	0.58897386
3	modelC_2A3C4E	0.00027	0.043770433	0.54975556
4	modelD_2A3C4E	0.00027	0.041642349	0.5202595

Table 3.4: Chisel nosecone results with varies of edge treatment.

NO	MODEL	FRONTAL AREA	DRAG FORCE	DRAG COEFFICIENT
1	modelD_2A3C4E	0.00027	0.041642349	0.5202595
2	modelD_2B3C4E	0.000265714	0.047875967	0.60778674
3	modelD_2C3C4E	0.00027	0.049195544	0.61462549

Table 3.5: Chisel nosecone results with varies of nose tip length.

NO	MODEL	FRONTAL AREA	DRAG FORCE	DRAG COEFFICIENT
1	modelD_2A3A4E	0.000269286	0.043520482	0.54516625
2	modelD_2A3B4E	0.00027	0.060379448	0.75435181
3	modelD_2A3C4E	0.00027	0.041642349	0.5202595
4	modelD_2A3D4E	0.00027	0.04717619	0.58304883
5	modelD_2A3E4E	0.00027	0.043507608	0.54356314

Table 3.6: Chisel nosecone results with varies of angles.

NO	MODEL	FRONTAL AREA	DRAG FORCE	DRAG COEFFICIENT
1	modelD_2A3C4A	0.000286456	0.050506793	0.59475861
2	modelD_2A3C4B	0.00027	0.044175254	0.55190439
3	modelD_2A3C4C	0.000286456	0.05140298	0.59989668
4	modelD_2A3C4D	0.000269286	0.045509446	0.57008132
5	modelD_2A3C4E	0.00027	0.041642349	0.5202595

This section compares and analyses the parametric quantitative studies of bullet nosecone and chisel nosecone.

The geometric parameters transformation methods employed for these two different shapes reveal their fundamental aerodynamic differences. Bullet nosecone exhibits a highly linear and monotonic trend, when the angle remains constant, the drag force and drag coefficient continuous increase with the increase of the nose tip radius. This predictable behaviour stems from the streamlined continuous curvature of the bullet shaped profile suppressing major flow separation, thus ensuring that any increase in aerodynamic drag is strictly proportional to the expanded frontal stagnation zone and fluid surface friction. Conversely, chisel nosecone exhibits a highly non-linear multi-variable coupling effect [5]. Due to the model exhibits high complexity and sophistication in aerodynamics. Chisel nosecone involving four core geometric parameters, there is an extremely strong parameter coupling effect among there four variables. This means that any tiny local geometric change will not affect drag in isolation but will completely reconstruct the three-dimensional flow field around the front of the vehicle. Therefore, these 300 results of the chisel model seemingly discrete and fluctuating data sets are essentially a highly nonlinear, multivariate and complex system. Collective synergy can only be triggered when all parameters reach a specific aerodynamic equilibrium.

CONCLUSION

This study successfully investigated and evaluated the aerodynamic efficiency of bullet nosecone and chisel nosecone design parameters specifically designed for F1 in Schools applications. The goal was fully achieved through a systematic concept generation process utilizing morphological chart. By morphological chart cross-combining key parameters and following the Regulation 2025 F1 in Schools Racing Technical Regulation, total 325 models were successfully selected and subjected to analysis. CFD simulations were successfully performed using ANSYS Workbench software fluent analysis system at a standard racing speed of 22m/s. Analysis showed that even small geometric change significantly impacts overall aerodynamic drag. The bullet nosecone geometry (Model A_2E) was ultimately confirmed to provide optimal aerodynamic efficiency for the F1 in Schools. Quantitative evidence indicates that the continuous axisymmetric curvature of the bullet nosecone reduces aerodynamic drag by approximately 10.6% compared to the best performance of chisel nosecone design. Therefore, the bullet nose cone structure was determined to be the optimal solution for maximizing the performance of the F1 in Schools cars.

ACKNOWLEDGMENTS

The authors would like to express their gratitude to the Universiti Teknikal Malaysia Melaka for their contribution and encouragement in publishing scholarly works such as this article.

REFERENCES

1. M. N. A. M. D. K. I. M.H. Muhammad, "Optimising F1 in Schools Car Design: Using CFD Simulation and Wind Tunnel," Journal of Applied Engineering Design and Simulation, vol. 4, no. 1, 2024.
2. R. K. N. I. M. N. A. M. D. Mohd Hanif Mat Muhammad, "Optimising F1 in Schools Car Design Using CFD Simulation and Wind Tunnel Testing for Enhanced Aerodynamic Performance," JOURNAL OF APPLIED ENGINEERING DESIGN AND SIMULATION , vol. 4, no. 1, 2024.
3. F. Menter, "Two-equation eddy-viscosity turbulence models for engineering applications," AIAA JOURNAL, vol. 32, no. 8, 1994.
4. I. S. ANSYS, Ansys Fluent Theory Guide, Canonsburg, 2026.
5. J. R. R. A. M. A. Ning, Engineering Design Optimization, Cambridge, 2022.